Melt Polycondensation of Bisphenol A Polycarbonate by Forced Gas Sweeping Process II. Continuous Rotating-Disk Reactor

Boo-Gon Woo and Kyu Yong Choi*

Department of Chemical Engineering, University of Maryland, College Park, Maryland 20742

Kwang Ho Song

Chemical Process & Catalyst Research Institute, LG Chem Research Park, LG Chemical Ltd., 104-1 Moonji-dong, Yusong-gu, Taejon 305-380, Korea

Experimental and theoretical modeling studies are presented on the forced gas sweeping process for the continuous melt polycondensation of bisphenol A polycarbonate. In this process, unlike in the conventional high-vacuum melt polycondensation (transesterification) process, the condensation byproduct (phenol) is removed from a highly viscous polymer melt by forcing inert gas bubbles to flow directly through the polymer melt phase. As the gas bubbles rise in the polymer melt phase, dissolved phenol molecules diffuse to the bubbles and are removed from the polymer melt, and the polymer molecular weight increases. In this study, the feasibility of continuous reactor operation is investigated using a continuous rotating-disk reactor at 260−300 °C and ambient pressure. With a low-molecular-weight polycarbonate prepolymer (M_n = 5050) as the feed, polycarbonate of molecular weight up to 20 000 has been obtained at steady state. To investigate the effect of reactor operating conditions on the polymer molecular weight, a multicompartment dynamic mass-transfer reaction model has also been developed. In the model, bubble size and bubble rising velocity are used to estimate the interfacial mass-transfer area and average gas−liquid contact time. Both model simulations and experimental results indicate that the forced gas sweeping process can be a potential alternative to a high-vacuum continuous melt polycondensation process for the synthesis of bisphenol A polycarbonate.

Introduction

Polycarbonate is one of the top three engineering thermoplastic polymers, behind nylon and acrylonitrile−butadiene−styrene (ABS), with about 8−9% annual growth rate to meet growing global demand.[1] With its durability, optical clarity, and ability to be blended with other polymers, polycarbonate is used to make optical media formats, housings of electronic devices, and automotive parts.

To manufacture polycarbonate, interfacial phosgenation processes have been used industrially for many years. In this process, polycarbonate is produced by an interfacial polycondensation of bisphenol A with phosgene and sodium hydroxide between two solvents, methylene chloride and water, at about 40 °C. However, this process has problems in that toxic phosgene is used and process equipment can become corroded with chlorine-containing compounds such as hydrogen chloride, sodium chloride, and methylene chloride. The separation and removal of impurities after polymerization is also costly. Thus, there is an increasing industrial interest in and need for manufacturing polycarbonate by environmentally other, more benign polymerization techniques such as melt transesterification processes that do not use phosgene gas. The melt process is attractive in that a solvent or toxic monomer is not used. Also, the purity of melt-phase polycarbonate is known to bring major benefits in high-growth optical media and automotive glazing markets. In recent years, an increasing number of major polycarbonate producers have started commericializing the melt polycondensation processes.

In a typical melt polycondensation process, bisphenol A (4,4-dihydroxydiphenyl-2,2-propane) and diphenyl carbonate are polymerized at 260−300 °C in a molten state in the presence of catalyst such as $LiOH·H_2O$. The polymerization process consists of a prepolymerization stage and a finishing polymerization stage. In the prepolymerization stage, bisphenol A and diphenyl carbonate are reacted at 180−250 °C to form a relatively low-molecular-weight prepolymer at reduced pressure using a stirred-tank-type reactor. The prepolymer is then transferred to a continuous finishing polymerization reactor such as a rotating-disk or screw reactor and polymerized further to obtain the higher-molecular-weight final polymer.

The main polycondensation reaction is a reversible reaction, and hence, the main reaction byproduct (phenol) should be removed from the increasingly viscous polymer melt to shift the equilibrium to a chain-growth reaction. To remove phenol in a conventional melt process, high vacuum (1−3 mmHg or less) is applied at 250−300 °C. The overall process characteristics are quite similar to those of polyester synthesis processes.

The performance of the melt process depends mainly on the efficiency of the removal of volatile condensation byproducts from the increasingly viscous polymer melt. In a high-vacuum melt process, the design of a continuous finishing-stage polymerization reactor is focused on the design of reactor internals that offer as large an interfacial mass-transfer area as possible per unit volume of polymer melt. It is also important that the temperature of the reacting melt phase be kept uniform

* To whom correspondence should be addressed.

10.1021/ie001150l CCC: $20.00
Published on Web 07/07/2001

in the reactor to avoid undesirable thermal degradation reactions. Various types of finishing reactors (e.g., wiped film reactors, rotating-disk reactors, screw reactors, etc.) have been developed for the melt polycondensation of aromatic polyesters and polycarbonates. However, a major drawback of the high-vacuum process is associated with its high equipment costs (vacuum equipment) and high energy costs in using high-pressure steam for steam jets.

In a high-vacuum melt process, the driving force for removal of phenol from the melt phase is the concentration difference between the melt phase and the gas−liquid interface. The mass-transfer area is provided by the reactor internals such as rotating disks, cages, and screws. To remove phenol from the polymer melt, an inert stripping gas can also be used instead of vacuum. Then, the volatile compounds in the melt phase are transferred to the gas phase and removed from the reactor.

The use of inert gas to remove condensation byproduct has been considered as a potential alternative to high-vacuum process in the past, particularly for polyester (e.g., PET) synthesis, albeit with no commercial realization. In the gas sweeping processes disclosed recently by Bhatia[2−4] for the synthesis of poly(ethylene terephthalate) (PET), an inert gas is supplied to a finishing reactor countercurrently to the flow of bulk melt polymer phase.

Even in patent literature, little has been reported on the use of inert gas for the melt polymerization of polycarbonate. One of the differences between the polyester (e.g., PET) and polycarbonate manufacturing processes is that the melt viscosity of a molten polycarbonate, particularly of high molecular weight, is much higher than the viscosity of polyesters. Alewelt et al.[5] disclosed a polycarbonate process in which prepolymer of molecular weight 2000−20 000 is passed through a heated tube (L/D = 10−200) while inert gas is also supplied to the tube reactor at a rate of 1 m^3/(kg of prepolymer). The resulting polymer molecular weight is about 15 000−60 000. Komiya et al.[6] disclosed a process in which prepolymer melt (M_w = 5000−9000) flows downward through a perforated plate and falls along a wire through a wire-wetting polymerization reaction zone. In their process, a small amount of inert gas, introduced from a pipe placed at the bottom of the reactor, flows upward. Thus, the gas and the polymer melt flowing down along the wires come into contact countercurrently. The reactor is operated at 250−280 °C under high vacuum (<1.0 mmHg). Polycarbonate of molecular weight of 6000−13000 were obtained. There are no reports that any of these processes have been commercialized.

Recently, Song et al.[7] disclosed a continuous melt polycondensation reactor system in which phenol is removed at 230−300 °C and ambient pressure by inert gas forced to flow through a polymer melt phase (forced gas sweeping process). Their reactor resembles a continuous rotating-disk reactor commonly used in high-vacuum processes, but it is equipped with a means for the injection of heated inert gas directly into the polymer melt. This process differs from other gas sweeping processes where inert gas flows in the bulk gas phase above the main body of the melt phase.[2−4] The direct injection of gas into the bulk melt phase and the flow of gas bubbles cause intense mixing of the melt phase, promoting higher reaction and mass-transfer rates. Song et al.[7] report that the molecular weight of polycarbonate prepolymers (M_w = 3000−20 000) is increased to 12 000−40 000 at steady state.

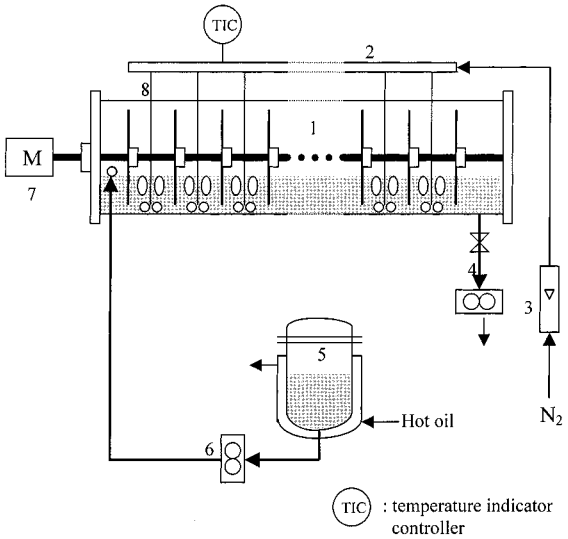

Figure 1. Experimental continuous polymerization reactor system: 1, polymerization reactor; 2, nitrogen gas preheater; 3, gas flow meter; 4, product withdrawal line; 5, prepolymer supply tank; 6, gear pump; 7, variable-speed motor; 8, dip tube for gas supply.

In our laboratory, we have investigated the mass-transfer and reaction phenomena in the polymerization of bisphenol A polycarbonate by the forced gas sweeping technique using a small glass tube reactor.[8,9] From our experimental study, it was confirmed that high-molecular-weight polycarbonate could readily be obtained at ambient pressure.

In this work, we present a new experimental and theoretical modeling study on the continuous polymerization of bisphenol A polycarbonate using the forced gas sweeping process (FGSP) described in Song et al.[7] Our main objective is to examine the applicability of the forced gas sweeping process to the synthesis of polycarbonate in a continuous melt polycondensation reactor.

Experimental Section

Based on the results of small-scale semibatch experimental studies on the forced gas sweeping process for polycarbonate synthesis reported in our previous paper,[8] a bench-scale continuous rotating-disk reactor system was constructed. Figure 1 illustrates the schematic diagram of the continuous reactor system used in our experiments. The reactor is a horizontal stainless steel cylindrical vessel (11.4 cm o.d. × 58.4 cm length) equipped with equally spaced flat disks mounted on a central shaft. The melt phase volume between the two adjacent disks constitutes a virtual reaction compartment, and there are 10 such compartments in the reactor. The rotating disks provide an overall plug-flow profile in the reactor system to minimize the axial mixing and, thereby, to obtain high-molecular-weight polymers. The basic structure of the reactor is very similar to that used in the conventional high-vacuum melt polymerization of aromatic polyesters (e.g., PET) and polycarbonates.[12−14] The main departure of the present reactor system from the conventional high-vacuum rotating-disk reactors is that inert nitrogen gas is injected directly into each reaction compartment through multiple ports to remove phenol produced by polymerization.

Pressurized and heated nitrogen gas is supplied to a gas supply hub from which gas is distributed to each reaction compartment through two stainless steel dip tubes of small diameter. The reactor is heated by electrical heating tapes wrapped around the reactor. Several preliminary experiments were performed to adjust the power supply to the heating tapes to obtain the desired reaction temperature profile in the reactor. A large amount of polycarbonate prepolymer (M_n = 5050) was first synthesized using a separate semibatch stirred-tank reactor with $LiOH \cdot H_2O$ as the catalyst following the experimental procedure described in ref 10.

To start a polymerization experiment, the polycarbonate prepolymer melted in a separate melting tank is supplied to the heated rotating-disk reactor by a gear pump. The polymer melt flow rate is held constant at 13.0 mL/min, and the volume of the polymer melt phase is 1.05 L (the mean residence time is about 80 min). After the reactor temperature is raised to the desired reaction temperature at steady melt flow rate, preheated and dehumidified nitrogen gas is supplied to the reactor through dip tubes at a constant flow rate (60 L/min). Nitrogen gas injected into the polymer melt phase flows through the polymer melt in the form of bubbles. As these bubbles rise in the melt phase, they induce intensive mixing of polymer melt in each compartment. A nitrogen and phenol vapor mixture is vented through the vent manifolds mounted at the top of the reactor (not shown in Figure 1). The glass sight windows installed on the reactor make visual observation of the bubbles and melt phase possible during the polymerization. The polymer melt is withdrawn continuously from the reactor outlet at a fixed flow rate by a gear pump. Three thermocouples were also installed to measure the melt temperatures at three different locations in the reactor. Because of limitations in the amount of prepolymer produced in our laboratory prepolymerization reactor, we were able to operate the reactor continuously for only 15 h. In our second series of experiments, another reactor with the same dimensions but with three heating jackets was used. The second reactor provides more uniform internal temperature profiles and eliminates potential thermal degradation reactions.

The molecular weight of polycarbonate was measured by gel permeation chromatography using five columns (two linear and three 500-Å columns) and a UV detector (254 nm) with tetrahydrofuran (THF) as the mobile phase.

Reactor Model

To analyze the performance of the continuous polymerization reactor used in our experimental study, a dynamic reactor model was developed. The basic configuration of the reactor system is illustrated schematically in Figure 1. A low-molecular-weight prepolymer melt containing an appropriate amount of polymerization catalyst (e.g., $LiOH \cdot H_2O$) is supplied to the reactor, and a heated, dehumidified nitrogen gas stream is injected through dip tubes into each compartment between two adjacent disks.

To model the reactor, we developed a multicompartment two-phase model (Figure 2) that is similar to the model developed by Cheong and Choi[14] for a high-vacuum PET process. It is assumed that the reactor consists of N reaction compartments, where a virtual

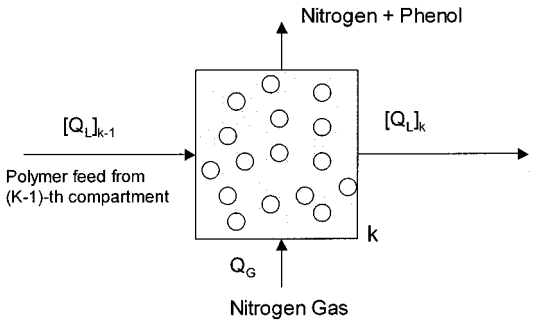

Figure 2. Multicompartment reactor model.

compartment is defined as the volume between two neighboring disks. In each compartment, we assume that the polymer melt phase is well-mixed by the rising gas bubbles, as observed in our semibatch experiments.[8] We also assume that phenol is mostly removed by the gas bubbles and that the amount of phenol removed from the polymer layers at the surfaces of the rotating disks is negligibly small. It is also assumed that the polymer melt and gas holdups are uniform from compartment to compartment and that the melt flow rate in each compartment is also the same and constant.

It is possible that the viscosity of the polymer might affect the actual nitrogen gas flow rate in each compartment. However, we assume that the gas flow rate in each compartment is the same. The inert gas flows through the polymer melt phase as bubbles. Phenol, produced by the polycondensation reaction, diffuses to the gas−liquid interface and is absorbed into the gas bubbles. As the polymer melt flows toward the outlet of the reactor, the polymer molecular weight and the melt viscosity increase. The effectiveness of the reactor operation is certainly dependent on the gas−liquid mass-transfer area created by the rising gas bubbles. The melt viscosity in the reactor affects the size of the gas bubbles and the bubble rising velocity.

Although some side reactions (e.g., Kolbe−Schmitt reactions) might occur in a high-temperature melt polycondensation reactor, we consider only the main polycondensation reaction in this study. The polymerization occurs reversibly by the reaction between hydroxyl group (E_A) and phenyl carbonate group (E_B) as follows

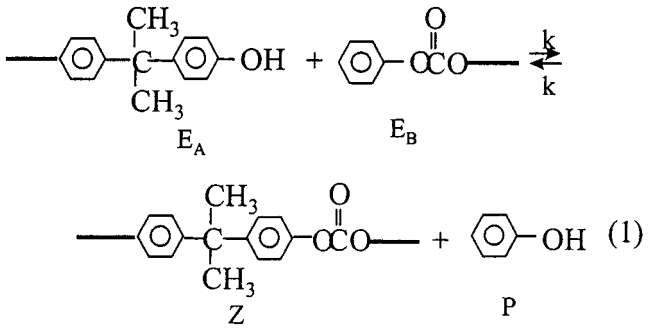

(1)

where E_A and E_B denote hydroxyl and phenyl carbonate groups, respectively. Z is the polymer repeat unit, and P is phenol. The reaction rate is expressed as

$$r = k[E_A][E_B] - k'[Z][P] \qquad (2)$$

The above reaction reaches an equilibrium unless phenol is removed from the reaction mixture. To remove phenol, either vacuum or inert gas can be used.

The molar transfer rate of phenol from the polymer melt phase to the nitrogen gas bubbles can be represented by

$$N_p = (k_L a)_L([P]_L - [P]_L^*) = (k_L a)_G([P]_G^* - [P]_G) \quad (3)$$

where $(k_L a)_L$ and $(k_L a)_G$ are the mass-transfer coefficients of phenol in the polymer melt phase and the nitrogen gas phase, respectively (a = specific interfacial surface area per liquid volume). $[P]_L$ ($[P]_G$) is the concentration of phenol in the liquid phase (gas bubble phase), and [P]* is the corresponding equilibrium concentration at the gas−liquid interface. The equilibrium concentrations of phenol at the gas−liquid interface are related by the equation

$$[P]_G^* = K[P]_L^* \quad (4)$$

If the mass-transfer resistance in the gas phase is much smaller than that in the polymer phase, eqs 3 and 4 are reduced to

$$N_p = (k_L a)_L\left([P]_L - \frac{1}{K}[P]_G\right) \quad (5)$$

Then, the mass balance equations for the kth compartment take the following form

$$\frac{d[E_A]_k}{dt} = -r_{p,k} + (Q_L/V_L)([E_A]_{k-1} - [E_A]_k) \quad (6)$$

$$\frac{d[E_B]_k}{dt} = -r_{p,k} + (Q_L/V_L)([E_B]_{k-1} - [E_B]_k) \quad (7)$$

$$\frac{d[Z]_k}{dt} = r_{p,k} + (Q_L/V_L)([Z]_{k-1} - [Z]_k) \quad (8)$$

$$\frac{d[P]_{L,k}}{dt} = r_{p,k} - k_L a([P]_{L,k} - [P]_G/K) + (Q_L/V_L)([P]_{L,k-1} - [P]_{L,k}) \quad (9)$$

$$\frac{d[P]_{G,k}}{dt} = (V_L/V_G)\cdot k_L a([P]_{L,k} - [P]_{G,k}/K) - (Q_G/V_G)[P]_{G,k} \quad (10)$$

where $r_{p,k}$ is the reaction rate in the kth compartment and $[E_A]_k$ and $[E_B]_k$ are the molar concentrations of hydroxyl and phenyl carbonate end groups in the kth compartment, respectively. $[P]_{L,k}$ is the molar concentration of phenol in the polymer melt phase in the kth compartment. $[P]_{G,k}$ is the molar concentration of phenol in the nitrogen gas bubble phase in the kth compartment. Q_L is the volumetric melt flow rate, V_L is the melt phase volume in each compartment, and V_G is the gas holdup in each compartment. Although phenol is removed from each compartment, we assume that the melt phase holdup (V_L) is approximately constant. In the above model, the same inert gas flow rate (V_G) is also assumed in each compartment.

Two of the key parameters in the above model are the mass-transfer coefficient (k_L) and the specific interfacial mass-transfer area (a). The mass-transfer coefficient is estimated using penetration theory as $k_L = 2\sqrt{D_p/\pi\theta}$, where D_p is the diffusivity of phenol in the polymer melt and θ is the contact time between the bubble and the melt phase at the gas−liquid interface. The diffusivity of phenol in the polymer melt phase is represented by the equation[9]

$$D_p(T) = 5.440 \times 10^{14} \exp\left(\frac{-23887.8}{T}\right) \quad (\text{cm}^2/\text{s},\ T \text{ in K}) \quad (11)$$

Estimating the specific gas−liquid interfacial area as a function of gas injection rate and the properties of the polymer melt is a difficult problem. It is also experimentally very difficult to measure the specific interfacial area because the polymerization reaction occurs in the melt phase, changing the rheological properties of the polymer melt. The formation of gas bubbles and their behavior in viscous liquids have been the subject of studies by many researchers in many different technical fields (e.g., fermentation, drying of liquid foodstuffs, wastewater treatment, polymer devolatilization, etc.). Predictions of bubble size, bubble growth, and bubble rising velocity in a highly viscous or viscoelastic fluid are important for process design. However, such phenomena are quite complex, and not much has been reported on the formation and movement of bubbles in high-viscosity polymer melts. In addition, no reports are available on bubble formation and growth in a reactive polymer melt where the melt viscosity increases significantly with conversion or time.

The specific mass-transfer interfacial area (a) provided by the gas bubbles is estimated from the bubble holdup and the bubble size. When gas is injected into a viscous liquid through an orifice, bubble size is a function of the orifice size at low gas flow rates. As the gas flow rate is increased to a certain point, bubble formation is hindered by the presence of preceding bubbles, and bubble size increases as a function of gas flow rate and melt viscosity rather than depending on the orifice size. In our experiments, the gas flow rates employed are such that bubbles are far larger than the diameter of the gas injection tube. In our previous report on semibatch polymerization with similar reaction conditions,[8] it was observed that the bubbles are significantly deformed at high viscosities. For example, at low viscosity, the bubbles are nearly spherical, whereas at high viscosity, the bubbles are elongated vertically and are more or less of cylindrical shape. In our modeling, however, we assume that all of the bubbles are spherical. For fluids with very low Reynolds numbers ($Re < 0.002$), Davidson and Schüler[15] proposed the following equation to estimate the volume of a gas bubble (V_G^*) in a viscous liquid when the volumetric gas flow rate is Q_G

$$V_G^* = \left(\frac{4\pi}{3}\right)^{1/4}\left(\frac{15\nu Q_G}{2g}\right)^{3/4} \quad (12)$$

where ν is the kinematic viscosity of the liquid and g is the gravitational acceleration (980 cm/s^2). Equation 12 indicates that the bubble volume increases as the melt viscosity increases. In other words, the bubble size and the gas−liquid mass-transfer area change from compartment to compartment as the polymer molecular weight and melt viscosity increase. In deriving eq 12, Davidson and Schüler assumed that (i) the bubble is spherical throughout formation, (ii) the liquid surrounding the orifice is at rest when the bubble starts to form, (iii) the motion of the gas bubble is not affected by the presence of another bubble immediately above it, (iv) the momentum of the gas is negligible, and (v) the

bubble is at all instants moving at the Stokes velocity appropriate to its size. In our polymerization system, some of these assumptions might not be exactly applicable. For example, Davidson and Schüler tested the above equation for fluids with viscosities up to only 1040 cP, which is far smaller than the viscosity of the polycarbonate melt in our polymerization system (up to 10^4 P[8]). Also, bubbles detached from the tip of a gas injection tube are nearly spherical at low melt viscosities, but as the melt viscosity increases because of polymerization, the bubbles become inflated and elongated in the vertical direction (bubble flow direction).[8]

The polycarbonate melt viscosity depends on the temperature and molecular weight, and the following correlation is used in our modeling[16]

$$\ln \mu = \left(393.15 - \frac{2.43 \times 10^5}{T}\right) + \left(\frac{2.49 \times 10^4}{T} - 39.8\right) \ln \bar{M}_w \quad (\mu \text{ in poise}) \quad (13)$$

where T is the melt temperature (in K) and $\bar{M}_w$ is the weight-average molecular weight of the polycarbonate. We also assume that the increase in the bubble size due to the diffusion of phenol from the melt phase to the gas bubbles is negligible because the bubble−melt contact time is quite small and the amount of phenol in the rapidly rising bubbles is also quite small. The change in bubble size due to bubble breakup or coalescence is also ignored.

Another important variable for the estimation of the bubble surface area and contact time is the bubble rising velocity. For a power-law fluid, Chhabra[17] reports that, depending on the values of power law fluid index (n) and the gas volume fraction, the rise velocity of a bubble swarm might be greater or smaller than the velocity of a single bubble. To estimate the bubble rising velocity for a vertical bubble stream rising with a stationary velocity in a viscous liquid, we use the equation proposed for a viscous liquid by Snabre and Magnifotcham[18]

$$u_b = \left[\frac{2 d_b g}{C_d}\left(1 + \frac{Q_G d_b}{u_b V_G^*}\right)\right]^{1/2} \quad (14)$$

where d_b is the bubble diameter (cm) and C_d is the drag coefficient ($C_d = 16/Re + 1$).

To determine the gas−liquid (melt) contact time (θ), the average residence time of the rising bubbles in the melt phase needs to be estimated. For a constant melt phase volume, the average bubble residence time (or contact time) in the reactor and the number of bubbles (N_b) with average residence time of θ are estimated using the equations

$$\theta = \frac{h_R}{u_b} \quad (15)$$

$$N_b = \frac{Q_G \theta}{V_G^*} \quad (16)$$

respectively, where h_R is the height of melt phase above the gas injection point. Figure 3 shows the frequency of bubble detachment from a gas injection tube measured in our small glass tube reactor.[8,9] Notice that the bubble detachment frequency decreases significantly with reaction time, and thus the number of bubbles generated

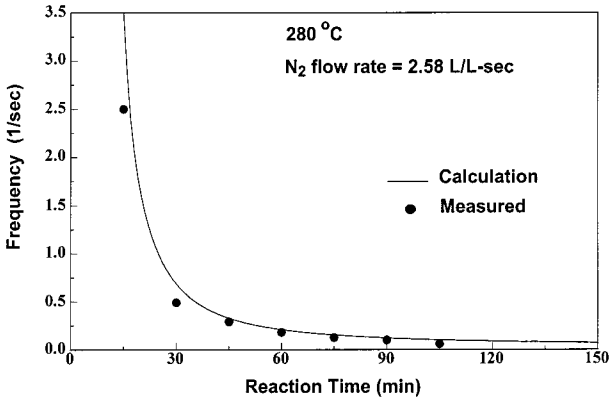

Figure 3. Frequency of bubble detachment in semibatch experiments.[8]

decreases accordingly. The specific mass-transfer area (a) is estimated by

$$a = \pi d_b^2 \left(\frac{N_b}{V_m}\right) \quad (17)$$

In the melt polymerization of bisphenol A polycarbonate, the reaction occurs even in the absence of added catalyst. The effective forward reaction rate constant is expressed as[10]

$$k = k_u + k_c[C^*] \quad (18)$$

where [C*] is the catalyst concentration (mol/L), k_u is the rate constant for the uncatalyzed polycondensation reaction, and k_c is the rate constant for the catalyzed reaction. The forward and reverse reaction rate constants for the uncatalyzed polycondensation are[10]

$$k_u = (5.180 \pm 0.170) \times 10^8 \times \exp[(-25\,290 \pm 1010)/RT] \ (\text{cm}^3\ \text{mol}^{-1}\ \text{s}^{-1}) \quad (19)$$

and

$$k'_u = (3.380 \pm 0.377) \times 10^{16} \times \exp[(-45\,030 \pm 2430)/RT] \ (\text{cm}^3\ \text{mol}^{-1}\ \text{s}^{-1}) \quad (20)$$

respectively. The corresponding catalyzed reaction rate constants are

$$k_c = 1.603 \times 10^{13} \exp[-13\,900/RT] \ (\text{cm}^6\ \text{mol}^{-2}\ \text{s}^{-1}) \quad (21)$$

and

$$k'_c = 1.340 \times 10^{12} \exp[-12\,090/RT] \ (\text{cm}^6\ \text{mol}^{-2}\ \text{s}^{-1}) \quad (22)$$

In the above expressions, the activation energies are in calories per mole, and the gas constant $R = 1.987$ cal $\text{mol}^{-1}\ \text{K}^{-1}$. The number-average degree of polymerization is given by

$$X_n = 1 + \frac{2[Z]}{[E_A] + [E_B]} \quad (23)$$

Results and Discussion

To assess the feasibility of continuous reactor operation, the polymerization experiment was first carried

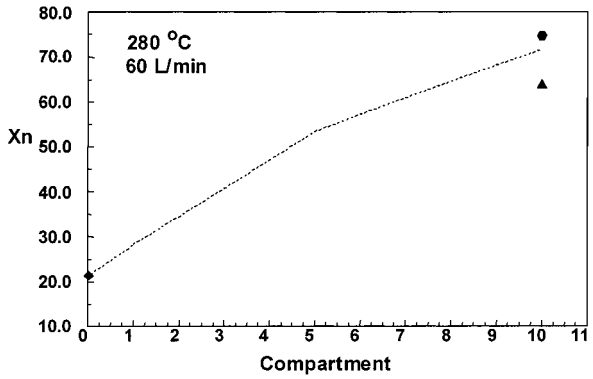

Figure 4. X_n profiles in the reactor at steady state: ▲, sample taken after 6 h; ⬢, sample taken after 12 h; dotted lines, simulations.

out at 280 °C using the electrically heated reactor. The actual temperature readings of the three thermocouples inserted at three different locations in the reactor were 278.3, 280.1, and 280.5 °C. However, because the temperature was measured inside the reactor, there was a possibility that the temperature at the inner surface of the reactor might have been higher than that measured in the bulk melt phase. A light brownish color of the product often observed in our experiments was believed to be an indication of such local temperature nonuniformity. The prepolymer feed flow rate was kept steady at 13.0 mL/min, and the nitrogen gas flow rate was fixed at 60 L/min. The initial end-group concentrations in the prepolymer were $[E_A] = 0.297$ mol/L, $[E_B] = 0.231$ mol/L, $[Z] = 5.583$ mol/L, and $[P] = 0.0058$ mol/L. In our model calculations, $K = 0.005$ is used. Because of the experimental complexity in operating the reactor system in our first series of experiments, only two samples were taken at the outlet of the reactor. A first polymer sample was taken after 6 h of operation (4.5 reactor residence times), and the second sample was taken after 12 h. The reactor was operated successfully without plugging for more than 15 h.

The model-calculated number-average degree of polymerization (X_n) in each compartment at 280 °C is shown in Figure 4. Also shown are the two experimentally measured values of X_n of the samples taken at the reactor outlet. The polymer sample taken after 12 h of operation (⬢) shows a slightly higher X_n value than the sample taken after 6 h (▲), but the difference is well within experimental errors. The mean residence time of the polymer melt in the reactor was 80 min. Therefore, these samples represent the steady-state molecular weight values. First, we see that a polymer molecular weight of 18 000 (M_n; $X_n = 71$) has been obtained from a prepolymer with a molecular weight 5050 ($X_n \approx 20$). The simulation results show that the polymer molecular weight increases almost linearly in each compartment. Considering the complexity of what is happening in the reactor (e.g., bubble formation, bubble movements, reaction, mass transfer, etc.), we think the model predictions are quite reasonable.

In the second series of experiments, we used a modified reactor with three sections of heating jackets for improved temperature control. The use of heating jackets eliminates the possible overheating problem at the reactor walls, which is often observed in electrically heated reactor systems. Figure 5 shows the plots of the steady-state X_n values at the outlet of the reactor at four different reaction temperatures with a gas flow rate of

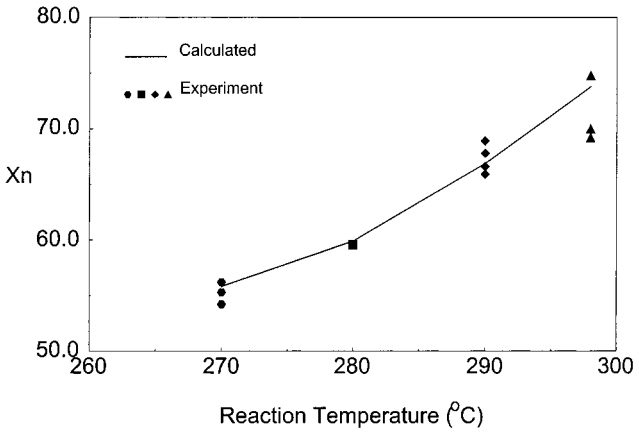

Figure 5. X_n profiles in the reactor (with heating jackets) at steady state; gas flow rate = 60 L/min.

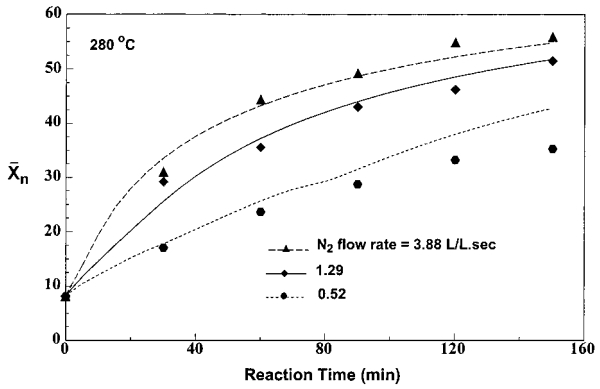

Figure 6. X_n vs reaction time profiles at 280 °C for three different gas flow rates (in liters of gas per liter of melt per second) in semibatch experiments.[8]

60 L/min. Notice that there is a strong temperature dependence of the molecular weight. Also, the agreement between the data and the model predictions is quite satisfactory, particularly considering some uncertainties in the model parameters taken from the empirical correlations reported in the literature.

For comparison, Figure 6 shows similar plots of the X_n values observed in semibatch polymerization experiments.[8,9] Note that the prepolymer molecular weight used in the semibatch experiments shown in Figure 6 is lower than the molecular weight of the prepolymer used in the continuous polymerization experiment. The gas flow rate of 1.29 L/(L s) in the semibatch experiment is close to the gas flow rate employed in the continuous reaction experiments. In the semibatch experiment (Figure 6), the X_n value increased from about 20 to 44 in 80 min. The relative increase in the polymer molecular weight (X_n/X_{n0}) after 80 min (one residence time of the continuous reactor) is higher in the continuous polymerization ($X_n/X_{n0} = 3.5$) than in the semibatch polymerization ($X_n/X_{n0} = 2.2$), indicating that the continuous polymerization is more efficient [X_{n0} is the reference degree of polymerization (e.g., prepolymer)]. In the semibatch experiments using the small glass tube reactor (diameter = 1.8 cm),[8,9] the population of gas bubbles in the melt phase was much smaller, and the gas−liquid contact time was also shorter. As a result, the total interfacial area was smaller, and the overall rate of mass transfer was smaller than in the continuous polymerization reactor, where two gas injection tubes were used per compartment. The changes in X_n value with reaction time in several compartments are shown

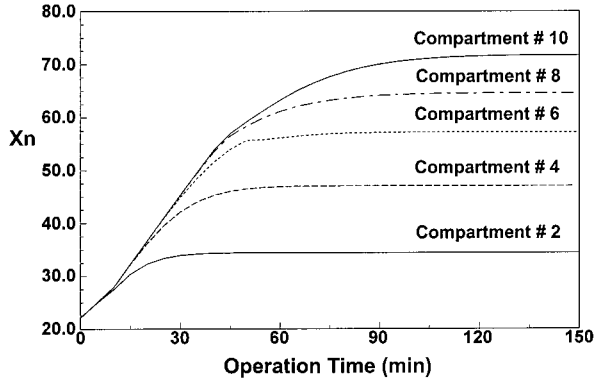

Figure 7. Degree of polymerization vs reaction time profiles in reaction compartments (280 °C, 60 L/min).

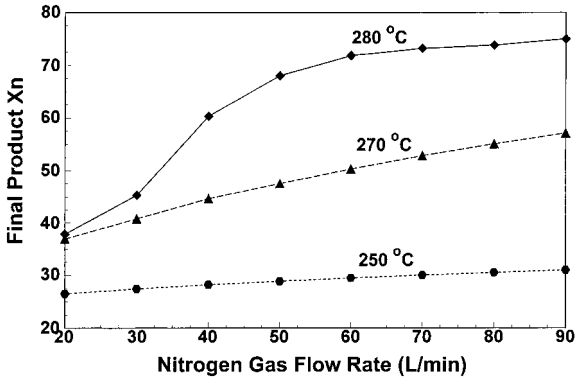

Figure 8. Effects of gas flow rate and reaction temperature on polycarbonate molecular weight at reactor exit (simulations).

in Figure 7. It is seen that the reactor reaches a steady state in about 80−90 min.

The effects of gas flow rate and reaction temperature on polymer molecular weight at steady state are shown in Figure 8 (model simulations). It is seen that the effect of gas flow rate on the X_n value of the final polycarbonate product is quite strong at gas flow rates below 50 L/min, particularly at 280 °C, but at gas flow rates larger than 50 L/min, the polymer molecular weight increases only slightly. This phenomenon suggests that there is a certain upper limit to the gas flow rate above which the additional increases in the gas flow rate are no longer effective. It is also observed that, at low reaction temperature (250 °C), the polymer molecular weight increase is only marginal even at very high gas flow rates, indicating that the gas sweeping process is not quite effective at such low temperatures because of low reaction rates.

The calculated bubble rising velocity and melt viscosity in each compartment are shown in Figure 9. It is seen that the bubble rising velocity decreases dramatically along the direction of melt flow as the polymer melt viscosity increases. However, at about the fifth compartment, the bubble rising velocity becomes quite small, and the rate of increase in the melt viscosity also declines. A slight break in the X_n profile in Figure 4 is probably due to this effect. Notice that the calculated melt viscosity at the reactor outlet reaches as high as 30 000 P. Figure 10 illustrates the calculated interfacial mass-transfer area [$cm^2/(cm^3$of melt)] in each compartment. The simulation results suggest that a larger number of small bubbles are formed at low conversion and that they rise rapidly in the lower-numbered compartments ($n < 5$), whereas a few huge bubbles are formed and rise very slowly in the higher-numbered

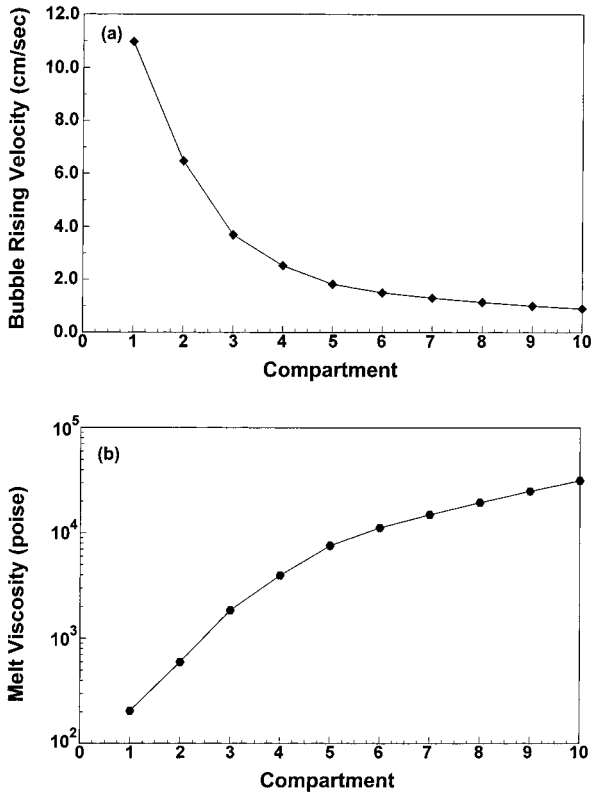

Figure 9. Bubble rising velocity and melt viscosity at 280 °C and a gas flow rate of 60 L/min (simulations).

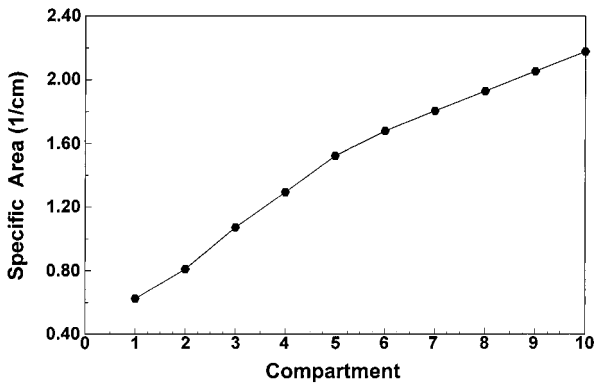

Figure 10. Calculated specific interfacial mass-transfer area in each compartment (280 °C, gas flow rate = 60 L/min).

compartments ($n > 5$). Such phenomena were observed visually through the sight glasses on the upper part of the reactor during the polymerization experiments. The mass transfer of phenol in the polymer melt is most effective when the nitrogen gas bubbles are not limited by the structure of the reactor because a spherical gas bubble has the largest interfacial area for the same gas volume. Therefore, one can optimize the minimum length between two adjacent disks. For example, the distance between the rotating disks can be adjusted to accommodate increasing bubble size and, hence, to increase the rate of mass transfer.

Concluding Remarks

A multicompartment dynamic mass-transfer reaction model has been developed for the analysis of the continuous melt polycondensation of bisphenol A polycarbonate by a forced gas sweeping process, and the feasibility of the process has been examined through

experimentation. Although an extensive parametric study has not been carried out experimentally, our experimental and theoretical modeling studies suggest that the forced gas sweeping process can be applied to the continuous production of bisphenol A polycarbonate at ambient pressure.

From the experimental and simulation results, it was shown that both the reaction temperature and the nitrogen gas flow rate are two of the most important reaction conditions for obtaining high-molecular-weight polycarbonate. At low temperatures (e.g., 250 °C), the process is chemical-reaction-controlled, and the use of very high gas flow rate fails to produce high-molecular-weight polymer. Therefore, it is very important to keep the reaction temperature high enough to achieve high-molecular-weight polycarbonate. It has also been shown through model simulations that there is an upper limit to the gas flow rate above which the mass-transfer rate is no longer dependent on the gas flow rate. Thus, from the process design point of view, we can say that, for a given reactor size or configuration, one needs to identify the optimal gas flow rate and reaction temperature for obtaining high-molecular-weight polycarbonate in the shortest reaction time. One can think of several other design parameters such as the number of gas injection points per compartment, the compartment size, the bulk phase melt holdup, etc. that yield the most economical process operating conditions.

Acknowledgment

We are indebted to LG Chemical Company for the financial support of this work.

Nomenclature

a = interfacial surface area (cm^{-1})
d_b = bubble diameter (cm)
C_d = drag coefficient
D_p = diffusivity of phenol in polycarbonate ($cm^2\ s^{-1}$)
$[E_A]$ = concentration of terminal hydroxyl group (mol L^{-1})
$[E_B]$ = concentration of terminal phenyl carbonate group (mol L^{-1})
g = acceleration of gravity (cm s^{-2})
h = height of melt phase above gas injection point (cm)
k_c = rate constant for catalyzed reaction ($cm^3\ mol^{-1}\ s^{-1}$)
k_L = mass-transfer coefficient (cm s^{-1})
k_u = rate constant for uncatalyzed reaction ($cm^3\ mol^{-1}\ s^{-1}$)
K = vapor−liquid equilibrium coefficient
$\bar{M}_n$ = number-average molecular weight (g mol^{-1})
$\bar{M}_w$ = weight-average molecular weight (g mol^{-1})
N_b = number of gas bubbles
N_p = molar transfer rate of phenol (mol $cm^{-3}s^{-1}$)
[P] = concentration of phenol (mol cm^{-3})
[P]* = concentration of phenol at gas−liquid interface (mol cm^{-3})
Q_G = gas flow rate ($cm^3\ s^{-1}$)
Q_L = liquid (melt) flow rate ($cm^3\ s^{-1}$)
Re = Reynolds number
r_p = rate of polymerization (mol $L^{-1}\ min^{-1}$)
S_G^* = surface area of a gas bubble (cm^2)
T = temperature (K)
u_b = bubble rising velocity (cm s^{-1})
V_G = total volume of gas bubbles (cm^3)
V_G^* = volume of single gas bubble (cm^3)
V_L = melt phase volume (cm^3)
$\bar{X}_n$ = number-average degree of polymerization
$\bar{X}_w$ = weight-average degree of polymerization
[Z] = concentration of polycarbonate repeating unit (mol L^{-1})

Greek Letters

μ = melt viscosity (g $cm^{-1}\ s^{-1}$)
ν = kinematic viscosity ($cm^2\ s^{-1}$)
θ = gas−liquid contact time (s)

Subscripts

b = bubble
G = gas phase
L = liquid (melt) phase

Literature Cited

(1) Tullo, A. H. Fighting for Position in Polycarbonate. *Chem. Eng. News* **2001**, *79*, 15−16.

(2) Bhatia, K. K. Polyester Production Process. U.S. Patent 5,688,898, 1997.

(3) Bhatia, K. K. Polyester Production Process. U.S. Patent 5,849,849, 1998.

(4) Bhatia, K. K. Polyester Production. U.S. Patent 5,856,423, 1999.

(5) Alewelt, W.; Kanth, H.; Kühling, S. Process for the Production of Polycarbonates. U.S. Patent 5,384,389, 1995.

(6) Komiya, K.; Kawakami, Y.; Okamoto, H. Wire-Wetting Fall Polymerization Process for the Production of Polycarbonate. U.S. Patent 5,589,564, 1996.

(7) Song, K. H.; Lee, S. H.; Park, K. H. Process for the manufacturing of polycarbonate. Korean Patent 1999-73161, 1999.

(8) Woo, B.-G.; Choi, K. Y. Melt Polycondensation of Bisphenol A Polycarbonate by Forced Gas Sweeping Process. *Ind. Eng. Chem. Res.* **2000**, *40* (5), 1312−1319.

(9) Woo, B.-G. The Mass Transfer and Reaction Phenomena in Melt Polycondensation Processes. Ph.D. Thesis, University of Maryland, College Park, MD, 2000.

(10) Kim, Y. S.; Choi, K. Y. Multistage melt polymerization of bisphenol A and diphenyl carbonate to polycarbonate. *J. Appl. Polym. Sci.* **1993**, *49*, 747−764.

(11) Ravindranath, K.; Mashelkar, R. A. Finishing Stages of PET Synthesis: A Comprehensive Model. *AIChE J.* **1984**, *30* (3), 415−422.

(12) Laubriet, C.; LeCorre, B.; Choi, K. Y. Two-Phase Model for Continuous Final Stage Melt Polycondensation of Poly(ethylene terephthalate) I. Steady-State Analysis. *Ind. Eng. Chem. Res.* **1991**, *29* (1), 2−12.

(13) Castres Saint Martin, H.; Choi, K. Y. Two-Phase Model for Continuous Final Stage Melt Polycondensation of Poly(ethylene terephthalate) II. Analysis of Dynamic Behavior. *Ind. Eng. Chem. Res.* **1991**, *30*, 1712−1718.

(14) Cheong, S. I.; Choi, K. Y. Modeling of a Continuous Rotating Disk Polycondensation Reactor for the Synthesis of Thermoplastic Polyesters. *J. Appl. Polym. Sci.* **1996**, *61* (5), 763−773.

(15) Davidson, J. F.; Schüler, B. O. G. Bubble Formation at an Orifice in a Viscous Liquid. *Trans. Inst. Chem. Eng.* **1960**, *38*, S105−S115.

(16) Schnell, H. *Chemistry and Physics of Polycarbonates*; Interscience: New York, 1964; p 123.

(17) Chhabra, R. P. Rising Velocity of a Swarm of Spherical Bubbles in Power Law Fluids at High Reynolds Number. *Can. J. Chem. Eng.* **1998**, *76*, 137.

(18) Snabre, P.; Magnifotcham, F. Formation and rise of a bubble stream in a Viscous liquid. *Eur. Phys. J.* **1998**, *B4*, 369−377.

Received for review December 30, 2000
Revised manuscript received June 6, 2001
Accepted June 6, 2001

IE001150L